Provided academic cases

Michaël TOUATI

11 August 2021

Abstract

Four well-known Plasma Physics academic cases are provided with ESVM:

1. the emission of an electrostatic wakefield by a Gaussian electron; cf. Figure 1
2. the linear Landau damping of an electron plasma wave; cf. Figure 2,
3. the non-linear Landau damping of an electron plasma wave; cf. Figure 3 and
4. the two-stream instability of two counter-propagating symmetric Gaussian electron beams; cf. Figure 4.

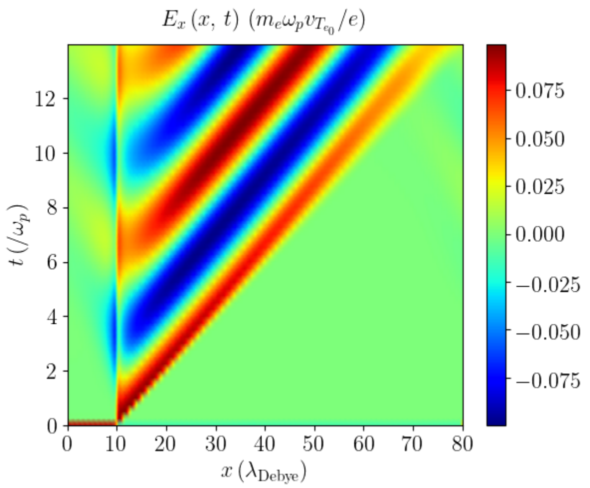

Figure 1: Electrostatic wakefield $E_x(x,t)$ emitted by a Gaussian electron propagating in a collisionless plasma at Maxwell-Boltzmann equilibrium (1) and initialized according to (2) with $A = 0.1$ and $\underline{v_d} = 5$.

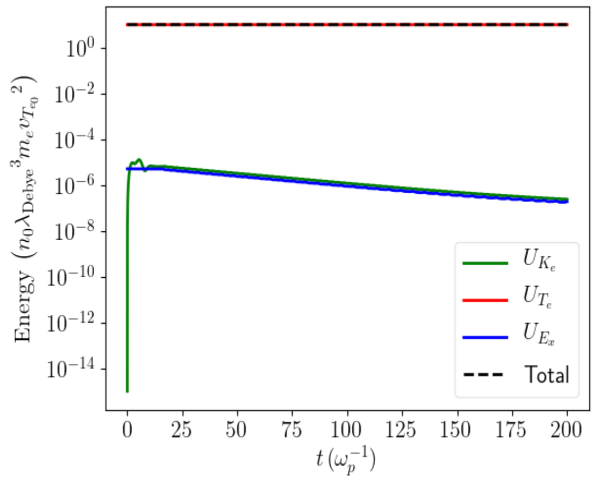

Figure 2: Total electrostatic field energy and plasma electrons kinetic energy in the linearly Landau damped electron plasma wave propagating in the collisionless plasma at Maxwell-Boltzmann equilibrium (1) and initialized according to (3) with $A = 10^{-3}$, $\underline{k} = 0.29919930034$ and $\underline{\omega_0} = 1.18$.

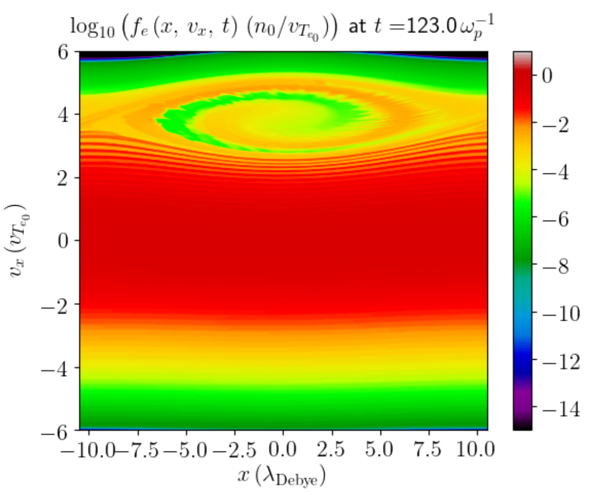

Figure 3: Plasma electrons phase-space $\underline{f_e}(\underline{x}, \underline{v_x}, \underline{t} = 68)$ in the non-linear Landau damping of the electron plasma wave propagating in the collisionless plasma at Maxwell-Boltzmann equilibrium (1) and initialized according to (3) with $A = 10^{-1}$, $\underline{k} = 0.29919930034$ and $\underline{\omega_0} = 1.18$.

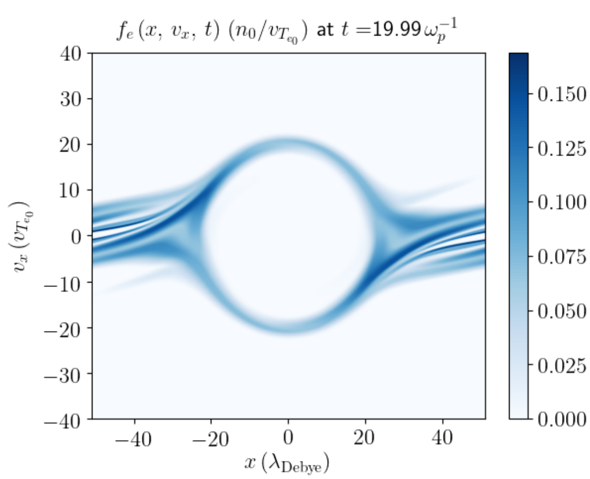

Figure 4: Plasma electrons phase-space $\underline{f_e}(\underline{x}, \underline{v_x}, \underline{t} = 19.99)$ in the two-stream instability of two counter-propagating electron beams initialized according to (8) with $A = 10^{-1}$, $\underline{k} = 0.06159985595$ ($\underline{x_{\min}} = -\underline{x_{\max}} = 51$) and $\underline{v_d} = 10$.

For each academic case, an example of input deck is provided together with one corresponding simulation result plot that the code typically generates. For 1), 2) and 3), the simulation is initialized assuming a non-drifting collisionless plasma at Maxwell-Boltzmann equilibrium

$$\left\{ \begin{array}{lll} f_e^{(0)}(x, v_x, t=0) & = & \frac{Zn_i}{\sqrt{2\pi {v_{T_{e_0}}}^2}} \exp\left[-\frac{{v_x}^2}{2{v_{T_{e_0}}}^2}\right] \\ E_x^{(0)}(x, t=0) & = & 0 \end{array} \right. \tag{1}$$

that is perturbed : - with a small perturbation

$$\delta f_e(x, v_x, t=0) = A\frac{Zn_i}{2\pi\delta x\delta v} \exp\left[-\frac{(x-x_d)^2}{2\delta x^2}\right] \exp\left[-\frac{(v_x-v_d)^2}{2\delta v^2}\right], \tag{2}$$

consisting in a Gaussian electron located at $x_d = x_{\min} + (x_{\max} - x_{\min})/8$ with a standard deviation $\delta x = \lambda_{\text{Debye}}/4$ and drifting at a velocity v_d with a standard deviation $\delta v = v_{T_{e_0}}/40$ at the simulation start $t = 0$ for 1), and - with a small perturbation consisting in a small amplitude electron plasma wave

$$\delta E_x(x, t < \delta t) = A\frac{m_e \omega_p v_{T_{e_0}}}{e} \sin(\omega_0 t - kx) \tag{3}$$

propagating during a short time interval $\delta t = 6\pi/\omega_0$ after the simulation start $t = 0$ for 2) and 3).

Only the perturbation amplitudes $A < 1$ for 1), 2) and 3), the perturbation drift velocity $v_d > v_{T_{e_0}}$ for 1) and the perturbation temporal and spatial angular frequencies ω_0 and k for 2) and 3) should be modified by the user when filling the input-deck in such a way that

$$\left\{ \begin{array}{lllll} f_e(x, v_x, t) & = & f_e^{(0)}(x, v_x, t) & + & \delta f_e(x, v_x, t) \\ E_x(x, t) & = & E_x^{(0)}(x, t) & + & \delta E_x(x, t) \end{array} \right. \quad \text{with } |\delta f_e(x, v_x, t)| \ll f_e^{(0)}(x, v_x, t) \tag{4}$$

keeps being respected during the linear stage of the simulation. Except for non-linear Plasma Physics processes such as 3) for which the non-linear theory should be considered [Sagdeev and Galeev, 1969], the methodology that can be used to check any ESVM simulation results is always the same. Only analytical estimates used to check the ESVM simulation results of the provided academic case 4) are consequently detailed here in order to highlight it. The user can check the provided academic case simulation results 1), 2) and 3) by directly comparing the ESVM simulation results with the analytical estimates provided in [Decyk, 1987] (available at https://picksc.idre.ucla.edu/wp-content/uploads/2015/04/DecykKyiv1987.pdf) and in the reference texbooks [Landau and Lifshitz, 1981] and [Sagdeev and Galeev, 1969], respectively.

The provided Plasma Physics academic case 4) is initialized assuming two counter-propagating homogeneous Gaussian electron beams '$e,+$' and '$e,-$' of exactly opposite drift velocity $\pm v_d$ with same standard deviation $v_{T_{e_0}}$

$$f_e^{(0)}(x, v_x, t) = f_{e,+}^{(0)}(x, v_x, t) + f_{e,-}^{(0)}(x, v_x, t) \tag{5}$$

with

$$f_{e,\pm}^{(0)}(x, v_x, t) = \frac{Zn_i/2}{\sqrt{2\pi {v_{T_{e_0}}}^2}} \exp\left[-\frac{(v_x \mp v_d)^2}{2{v_{T_{e_0}}}^2}\right] \tag{6}$$

that is a solution of the Vlasov Equation and that doesn't produce any electrostatic fields

$$E_x^{(0)}(x, t) = 0 \tag{7}$$

according to Maxwell-Gauss Equation. If one computes the Vlasov-Maxwell set of Equations exactly, initializing it with the two-stream equilibrium distribution function (5) without any perturbation, the counter-propagating electron beams would continue their propagation through the immobile plasma ions without any modification. In order to observe the two-stream instability,

$$f_e(x, v_x, t=0) = f_e^{(0)}(x, v_x, t=0) + \delta f_e(x, v_x, t=0), \tag{8}$$

is initialized instead by adding a small perturbation

$$\delta f_e(x, v_x, t=0) = \delta f_{e,+}(x, v_x, t=0) + \delta f_{e,-}(x, v_x, t=0) \tag{9}$$

on each beam of the form

$$\delta f_{e,\pm}(x, v_x, t=0) = \pm A \sin(k_1 x) f_{e,\pm}^{(0)}(x, v_x, t=0) \tag{10}$$

at the simulation start $t = 0$ with $A = 0.1$ and $k_1 = 2\pi/L_x$ (parameter k in the input-deck) that can be modified by the user in the input-deck where $L_x = x_{\max} - x_{\min}$.

In order to get analytical estimates of the exponentially growing electrostatic field, plasma electron density and mean velocity perturbations in this ESVM simulation, one can linearize the Vlasov equation and the self-consistent Maxwell-Gauss equation computed by ESVM assuming the perturbation (9) remains small compared to the equilibrium distribution (5) during the simulation. They read

$$\frac{\partial \delta f_e}{\partial t} + \frac{\partial}{\partial x}(v_x \delta f_e) - \frac{e}{m_e}\frac{df_e^{(0)}}{dv_x}\delta E_x = 0 \tag{11}$$

and

$$\frac{\partial \delta E_x}{\partial x} = -4\pi e \int_{-\infty}^{\infty} \delta f_e \, dv_x, \tag{12}$$

up to the first order. Considering periodic boundary conditions, we may use a one-sided Fourier transformation in time (thus equivalent to a Laplace transform) and a Fourier series expansion in space for such a L_x-periodic initial condition problem. We will note

$$\widehat{\mathrm{X}}_p(t) = \frac{1}{L_x}\int_0^{L_x} X(x,\, t)\exp(+\iota k_p x)dx \Leftrightarrow X(x,\, t) = \sum_{p=-\infty}^{\infty} \widehat{\mathrm{X}}_p(t)\exp(-\iota k_p x) \tag{13}$$

with $\forall p \in \mathbb{Z}$, $k_p = 2\pi p/L_x$ and

$$\begin{aligned} \widehat{\widehat{\mathrm{X}}}_p^{(+)}(\omega) &= \int_0^{\infty} dt \; \widehat{\mathrm{X}}_p(t) \; \exp(-\iota\omega t) \\ &= \int_0^{\infty} dt \int_0^{L_x} \frac{dx}{L_x} \; X(x,\, t) \; \exp[-\iota(\omega t - k_p x)] \\ \Leftrightarrow \quad X(x,\, t) &= \int_{\iota R-\infty}^{\iota R+\infty} \frac{d\omega}{2\pi} \sum_{p=-\infty}^{\infty} \widehat{\widehat{\mathrm{X}}}_p^{(+)}(\omega) \; \exp[+\iota(\omega t - k_p x)] \end{aligned} \tag{14}$$

where the integral in the complex ω-plane is taken along a straight line $\omega = \iota R$. By multiplying (11) and (12) by $\exp[-\iota(\omega t - k_p x)]/L_x$ and by integrating them from $x = 0$ to $x = L_x$ and from $t = 0$ to $t = \infty$, we obtain respectively

$$\widehat{\widehat{\delta \mathrm{f}}}_{e,p}^{(+)} = \frac{1}{\iota(\omega - k_p v_x)}\left[\widehat{\delta \mathrm{f}}_{e,p}(v_x,\, t=0) + \frac{e}{m_e}\frac{df_e^{(0)}}{dv_x}\widehat{\widehat{\delta \mathrm{E}}}_{x,p}^{(+)}\right] \tag{15}$$

with

$$\widehat{\delta \mathrm{f}}_{e,p}(v_x,\, t=0) = \alpha_p A \frac{Zn_i/2}{\sqrt{2\pi {v_{T_{e_0}}}^2}}\left\{\exp\left[-\frac{(v_x - v_d)^2}{2{v_{T_{e_0}}}^2}\right] - \exp\left[-\frac{(v_x + v_d)^2}{2{v_{T_{e_0}}}^2}\right]\right\} \tag{16}$$

where

$$\alpha_p = \begin{cases} \mp 1/2\iota & \text{if} \quad p = \pm 1 \\ 0 & \text{else} \end{cases} \tag{17}$$

and

$$\widehat{\widehat{\delta \mathrm{E}}}_{x,p}^{(+)} = \frac{4\pi e}{\iota k_p}\int_{-\infty}^{\infty} \widehat{\widehat{\delta \mathrm{f}}}_{e,p}^{(+)}(\omega,\, v_x)\, dv_x. \tag{18}$$

Injecting (15) in (18), we obtain the Fourier components of the electrostatic field Laplace transform

$$\begin{aligned} \widehat{\widehat{\delta \mathrm{E}}}_{x,p}^{(+)}(\omega) &= \frac{4\pi e}{{k_p}^2 \epsilon(\omega,\, k_p)}\int_{-\infty}^{\infty} \frac{\widehat{\delta \mathrm{f}}_{e,p}(v_x,\, t=0)}{v_x - \omega/k_p} dv_x \\ &= \alpha_p \frac{A}{2\sqrt{2}}\frac{m_e v_{T_{e_0}}}{e}\frac{\mathcal{Z}\left(\dfrac{\omega/k_p - v_d}{v_{T_{e_0}}\sqrt{2}}\right) - \mathcal{Z}\left(\dfrac{\omega/k_p + v_d}{v_{T_{e_0}}\sqrt{2}}\right)}{\epsilon(\omega,\, k_p)\,(k_p \lambda_{\mathrm{Debye}})^2} \end{aligned} \tag{19}$$

where the plasma electrical permittivity reads

$$
\begin{aligned}
\epsilon(\omega,\, k) &= 1-\frac{4\pi e^2}{m_e k^2}\int_{-\infty}^{\infty}\frac{1}{v_x-\omega/k}\frac{df_e^{(0)}}{dv_x}dv_x \\
&= 1+\frac{1}{(k\lambda_{\text{Debye}})^2}\left\{1+\frac{1}{2}\left[F\left(\frac{\omega/k-v_d}{v_{T_{e_0}}\sqrt{2}}\right)+F\left(\frac{\omega/k+v_d}{v_{T_{e_0}}\sqrt{2}}\right)\right]\right\}
\end{aligned} \tag{20}
$$

depending on the plasma dispersion function [Fried and Conte, 1961]

$$
F(\zeta)=\zeta\mathcal{Z}(\zeta) \text{ and } \mathcal{Z}(\zeta)=\frac{1}{\sqrt{\pi}}\int_{-\infty}^{\infty}\frac{\exp\left(-z^2\right)}{z-\zeta}dz. \tag{21}
$$

Since $v_d \gg v_{T_{e_0}}$ in this ESVM simulation, we have the condition

$$
\left|\frac{\omega}{k_p}\pm v_d\right| \gg v_{T_{e_0}}\sqrt{2} \tag{22}
$$

that is fulfilled for any given spatial frequency mode k_p and one thus may use the asymptotic limit

$$
F(\zeta) \underset{|\zeta|\gg 1}{=} \iota\zeta\sqrt{\pi}\exp\left(-\zeta^2\right)-1-\frac{1}{2\zeta^2}-\frac{3}{4\zeta^4}+O\left(\frac{1}{\zeta^6}\right) \tag{23}
$$

that leads to the simpler dispersion relation

$$
\epsilon(\omega,\, k) \underset{v_d\gg v_{T_{e_0}}}{=} 1-\frac{{\omega_p}^2}{2}\left[\frac{1}{(\omega-kv_d)^2}+\frac{1}{(\omega+kv_d)^2}\right]=0 \tag{24}
$$

retaining only the main term in the series expansion of the dispersion function (21) up to the second order (23). In this limit, the dispersion relation (24) provides four pure real solutions $\{\omega_1(k),\, \omega_2(k),\, \omega_3(k),\, \omega_4(k)\}\in\mathbb{R}^4$ for wavenumber k greater or equal than the critical wavenumber ω_p/v_d. It means that the two counter-propagating electron beams remain stable on space scales smaller than $2\pi v_d/\omega_p$. However, in the case where $k_p < \omega_p/v_d$ considered here, one finds in addition to the two real poles

$$
\omega_{1/2}\left(k<\frac{\omega_p}{v_d}\right)=\pm\omega_0(k) \tag{25}
$$

where

$$
\omega_0(k)=\omega_p\sqrt{\left(\frac{kv_d}{\omega_p}\right)^2+\frac{1}{2}\left(1+\sqrt{1+8\left(\frac{kv_d}{\omega_p}\right)^2}\right)} \underset{kv_d\ll\omega_p}{\sim} \omega_p, \tag{26}
$$

two another pure imaginary conjugate poles

$$
\omega_{3/4}(k<k_c)=\pm\iota\delta(k). \tag{27}
$$

It means that the two counter-propagating electron beams streaming throught the immobile plasma ions are unstable on space scales greater than $2\pi v_d/\omega_p$ and that this two-stream instability grows exponentially at the rate

$$
\delta(k)=\omega_p\sqrt{\frac{1}{2}\left(\sqrt{1+8\left(\frac{kv_d}{\omega_p}\right)^2}-1\right)-\left(\frac{kv_d}{\omega_p}\right)^2} \underset{kv_d\ll\omega_p}{\sim} |k|\, v_d. \tag{28}
$$

The stable electron plasma waves angular frequency (26) and the two stream instability growth rate (28) are plotted in Figure (5) as a function of the angular spatial frequency mode k. Retaining the main terms in the series expansions of $\mathcal{Z}$ up to the second order in (19) according to (23), the Fourier components of the electrostatic field Laplace transform simplify into

$$
\widehat{\widehat{\delta \mathrm{E}}}_{x,p}^{(+)}(\omega) \underset{v_d\gg v_{T_{e_0}}}{\sim} -\alpha_p A\frac{m_e v_d}{e}\frac{{\omega_p}^2}{\epsilon(\omega,\, k_p)(\omega-k_p v_d)(\omega+k_p v_d)}. \tag{29}
$$

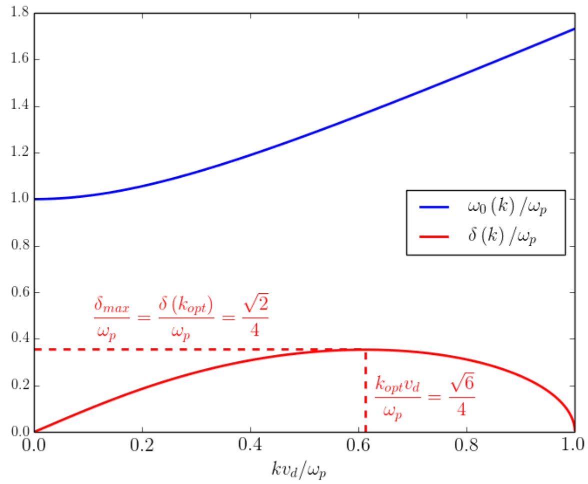

Figure 5: Two stream instability test case : Stationary electron plasma waves angular frequency (26) and the two-stream instability growth rate (28) as a function of the spatial angular frequency mode k.

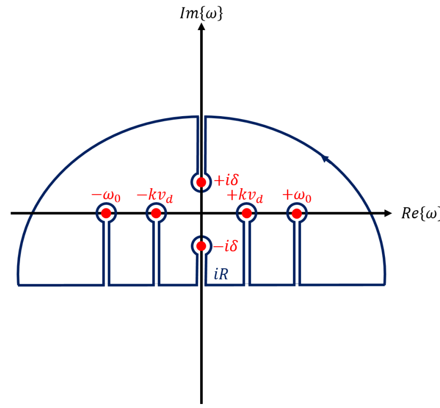

Figure 6: Two stream instability test case : Integration contour used to evaluate the the Cauchy principal value of the integral 30.

The poles of the Fourier components of the electrostatic fields (29) are thus $\pm k_p v_d$ plus the ones of the plasma electrical permittivity (24) given by Equations (25) and (27). We can know determine the time dependence of the spatial Fourier components of the growing electrostatic field

$$\widehat{\delta \mathrm{E}}_{x,p}(t) = \frac{1}{2\pi}\int_{\iota R-\infty}^{\iota R+\infty} \widehat{\widehat{\delta \mathrm{E}}}_{x,p}^{(+)}(\omega)\exp(+\iota\omega t)d\omega \tag{30}$$

by using the residue theorem with the contour illustrated in Figure 6 in order to evaluate the Cauchy principal value of this integral : since the function to integrate in 30 is an analytic function of ω defined in the whole complex plane, we moved the contour of integration usually taken slightly above the real axis into the lower half-plane sufficiently far beneath the pole $-\iota\delta$ and passing round this pole and round the other poles lying above it in such a way that it doesn't cross any of the poles of the function. We thus obtain

$$\begin{aligned} \widehat{\delta \mathrm{E}}_{x,p}(t) &= A \quad E_0 \quad \alpha_p \quad \frac{\omega_p}{\delta(k_p)} \quad \frac{\delta(k_p)^2 + (k_p v_d)^2}{\delta(k_p)^2 + \omega_0(k_p)^2} \quad \sinh[\delta(k_p)t] \\ &+ A \quad \frac{E_0}{2} \quad \alpha_p \quad \frac{\omega_p}{\omega_0(k_p)} \quad \frac{\omega_0(k_p)^2 - (k_p v_d)^2}{\delta(k_p)^2 + \omega_0(k_p)^2} \quad \sin[\omega_0(k_p)t] \end{aligned} \tag{31}$$

with

$$E_0 = \frac{m_e v_d \omega_p}{e} \tag{32}$$

that finally gives according to the Fourier series expansion (13)

$$\begin{aligned} \delta E_x(x,t) &= A \quad E_0 \quad \frac{\omega_p}{\delta(k_1)} \quad \frac{\delta(k_1)^2 + (k_1 v_d)^2}{\delta(k_1)^2 + \omega_0(k_1)^2} \quad \sinh[\delta(k_1)t]\sin(k_1 x) \\ &+ A \quad \frac{E_0}{2} \quad \frac{\omega_p}{\omega_0(k_1)} \quad \frac{\omega_0(k_1)^2 - (k_1 v_d)^2}{\delta(k_1)^2 + \omega_0(k_1)^2} \quad \sin[\omega_0(k_1)t]\sin(k_1 x). \end{aligned} \tag{33}$$

Knowing the electrostatic field (33), one may also deduce the perturbed distribution function according to (11). It reads

$$\begin{aligned} \delta f_e(x, v_x, t) &= \delta f_e(x, v_x, t=0) + \frac{e}{m_e}\frac{df_e^{(0)}}{dv_x}(v_x)\int_0^t \delta E_x[x + v_x(\tau - t), \tau]\,d\tau \\ &= f_{e,+}^{(0)}(v_x)\left[+A\sin(k_1 x) + \frac{v_d - v_x}{v_{T_{e_0}}^2}\frac{e}{m_e}\int_0^t \delta E_x[x + v_x(\tau - t), \tau]\,d\tau\right] \\ &+ f_{e,-}^{(0)}(v_x)\left[-A\sin(k_1 x) - \frac{v_d + v_x}{v_{T_{e_0}}^2}\frac{e}{m_e}\int_0^t \delta E_x[x + v_x(\tau - t), \tau]\,d\tau\right]. \end{aligned} \tag{34}$$

In the limit $k_p v_d \ll \omega_p$, they simplify into

$$\delta E_x(x,\,t) \underset{k_1 v_d \ll \omega_p}{\sim} A\frac{E_0}{2}\left[\sin(\omega_p t) + 4\frac{k_1 v_d}{\omega_p}\sinh(k_1 v_d t)\right]\sin(k_1 x) \tag{35}$$

and

$$\begin{aligned} & \frac{e}{m_e}\int_0^t \delta E_x\left[x + v_x(\tau - t)\,,\,\tau\right]d\tau \\ \underset{k_1 v_d \ll \omega_p}{\sim} \quad & A\frac{v_d}{1-\left(\dfrac{k_1 v_x}{\omega_p}\right)^2} \quad \left\{\frac{k_1 v_x}{\omega_p}\sin(\omega_p t) \quad \cos(k_1 x) - \left[\cos(\omega_p t) \quad - 1\right]\sin(k_1 x)\right\} \\ + \quad & A\frac{v_d}{1+\left(\dfrac{v_x}{v_d}\right)^2} \quad \left\{-\frac{v_x}{v_d}\,\sinh(k_1 v_d t)\cos(k_1 x) + \left[\cosh(k_1 v_d t) - 1\right]\sin(k_1 x)\right\}. \end{aligned} \tag{36}$$

We thus deduce in this limit

$$\begin{aligned} \delta n_e(x,\,t) \quad &= \quad \int_{-\infty}^{\infty} \delta f_e(x,\,v_x,\,t)\,dv_x \\ &\underset{k_1 v_d \ll \omega_p}{\sim} \quad -\frac{A}{2}Zn_i\frac{k_1 v_d}{\omega_p}\left[\sin(\omega_p t) + 4\frac{k_1 v_d}{\omega_p}\sinh(k_1 v_d t)\right]\cos(k_1 x) \end{aligned} \tag{37}$$

and

$$\begin{aligned} \delta v_e(x,\,t) \quad &= \quad \frac{1}{Zn_i}\int_{-\infty}^{\infty} v_x \delta f_e(x,\,v_x,\,t)\,dv_x \\ &\underset{k_1 v_d \ll \omega_p}{\sim} \quad -\frac{A}{2}v_d\left[\left(\cos(\omega_p t) - 1\right) + \left(2\frac{k_1 v_d}{\omega_p}\right)^2\left(\cosh(k_1 v_d t) - 1\right)\right]\sin(k_1 x). \end{aligned} \tag{38}$$

The first term in the square brackets

$$\left\{\begin{array}{lcccccc} \delta n_{\mathrm{osc}}(x,\,t) & \underset{k_1 v_d \ll \omega_p}{\sim} & -\dfrac{A}{2} & Zn_i\dfrac{k_1 v_d}{\omega_p} & \sin(\omega_p t) & \cos(k_1 x) \\ \delta v_{\mathrm{osc}}(x,\,t) & \underset{k_1 v_d \ll \omega_p}{\sim} & -\dfrac{A}{2} & v_d & \left(\cos(\omega_p t) - 1\right) & \sin(k_1 x) \\ \delta E_{\mathrm{osc}}(x,\,t) & \underset{k_1 v_d \ll \omega_p}{\sim} & \dfrac{A}{2} & E_0 & \sin(\omega_p t) & \sin(k_1 x) \end{array}\right. \tag{39}$$

corresponds to space-charge oscillations of stationary electrostatic plasma waves excited by the perturbation imposed on each electron beam. We are rather interested here in the second term in the square brackets

$$\left\{\begin{array}{lccccccc} \delta n_{\mathrm{ins}}(x,\,t) & \underset{k_1 v_d \ll \omega_p}{\sim} & -2A & Zn_i & \left(\dfrac{k_1 v_d}{\omega_p}\right)^2 & \sinh(k_1 v_d t) & \cos(k_1 x) \\ \delta v_{\mathrm{ins}}(x,\,t) & \underset{k_1 v_d \ll \omega_p}{\sim} & -2A & v_d & \left(\dfrac{k_1 v_d}{\omega_p}\right)^2 & \left(\cosh(k_1 v_d t) - 1\right) & \sin(k_1 x) \\ \delta E_{\mathrm{ins}}(x,\,t) & \underset{k_1 v_d \ll \omega_p}{\sim} & 2A & E_0 & \dfrac{k_1 v_d}{\omega_p} & \sinh(k_1 v_d t) & \sin(k_1 x) \end{array}\right. \tag{40}$$

corresponding to the exponentially growing electrostatic field due to the two-stream instability. These latter growing electron density, current density and electrostatic field perturbations (40) can directly be compared with the ESVM simulation result. One can also check that if $A = 0$, all quantities cancel. That confirms that, contrary to PIC codes, the two counter-propagating electron beams would continue their propagation without any modification if we do not impose an initial perturbation on which the instability will grow in ESVM. Finally, one can estimate the trajectories $(x_\ell,\,v_\ell)$ of one beam electron $\ell \in [1,\,N_e]$ with an arbitrary initial velocity $v_\ell(t=0) = v_0$ in the beam velocity distribution function and an initial position $x_\ell(t=0) = x_0$ close to $x = 0$ such that $k_1 x_0 \ll 1$. At the early stage of the instability, the growing electrostatic field component δE_{ins} is small compared to the stationary plasma wave δE_{osc} that oscillates in time at the Langmuir electron angular frequency ω_p. On such time scale $\omega_p t \sim 1$, the beam electrons are consequently mainly affected by this electrostatic field component

$$m_e\frac{dv_\ell}{dt} = -e\delta E_{\mathrm{osc}}\left(x_\ell(t)\,,\,t\right) \tag{41}$$

and their trajectory is thus given by

$$\frac{d^2 x_\ell}{dt^2} + {\omega_p}^2 \left(\frac{A}{2} \frac{k_1 v_d}{\omega_p} \right) \sin(\omega_p t) x_\ell(t) = 0, \tag{42}$$

assuming that $k_1 x_\ell(t) \ll 1$ remains valid at every time $t > 0$ if it is valid at $t = 0$ such that $\forall t$, $\sin[k_1 x_\ell(t)] \sim k_1 x_\ell(t)$. Recognizing the Mathieu Equation

$$\frac{d^2 x_\ell}{du^2} + [a - 2q\cos(2u)]\, x_\ell(u) = 0 \tag{43}$$

with $a = 0$ and $q = -Ak_1 v_d/\omega_p$ by doing the change of variable $u(t) = (-\pi/4) + (\omega_p t/2)$, we deduce

$$k_1 x_\ell(t) = k_1 x_c c_{e,0}[q,\, u(t)] + k_1 x_s s_{e,0}[q,\, u(t)] \tag{44}$$

and

$$v_\ell(t) = \frac{v_d}{2} \frac{\omega_p}{k_1 v_d} \left\{ k_1 x_c c'_{e,0}[q,\, u(t)] + k_1 x_s s'_{e,0}[q,\, u(t)] \right\} \tag{45}$$

with

$$\left\{ \begin{array}{rcl} k_1 x_c & = & +\dfrac{s'_{e,0}(q,\, -\pi/4)\, k_1 x_0 - s_{e,0}(q,\, -\pi/4)\,(2k_1 v_d/\omega_p)\,(v_0/v_d)}{c_{e,0}(q,\, -\pi/4)\, s'_{e,0}(q,\, -\pi/4) - c'_{e,0}(q,\, -\pi/4)\, s_{e,0}(q,\, -\pi/4)} \\ k_1 x_s & = & -\dfrac{c'_{e,0}(q,\, -\pi/4)\, k_1 x_0 - c_{e,0}(q,\, -\pi/4)\,(2k_1 v_d/\omega_p)\,(v_0/v_d)}{c_{e,0}(q,\, -\pi/4)\, s'_{e,0}(q,\, -\pi/4) - c'_{e,0}(q,\, -\pi/4)\, s_{e,0}(q,\, -\pi/4)} \end{array} \right. , \tag{46}$$

accounting for the initial conditions at $t = 0$. Here, $c_{e,a}(q,\, u)$ and $s_{e,a}(q,\, u)$ are respectively the even and odd solutions of Mathieu Equation (43) and $c'_{e,a}(q,\, u)$ and $s'_{e,a}(q,\, u)$ their first order derivatives. According to (44) and (45), the beam electron trajectories in space are only slightly modified compared to their ballistic initial trajectory $x_0 + v_0 t$ with a velocity that oscillates around their initial value v_0 with amplitudes slightly increasing with time. As a consequence, each beam velocity dispersion slightly increases with its propagation distance until the growing component of the electrostatic field δE_{ins} becomes greater than δE_{osc}. When this occurs, the equation of motion

$$m_e \frac{dv_\ell}{dt} = -e\delta E_{\mathrm{ins}}(x_\ell(t)\,,\, t) \tag{47}$$

gives

$$\frac{1}{2}\left(\frac{v_\ell(t)}{v_d}\right)^2 - \frac{1}{2}\left(\frac{v_0}{v_d}\right)^2 = -2Ak_1 \int_0^t v_\ell(t) \sin[k_1 x_\ell(t)] \sinh(k_1 v_d t) dt \tag{48}$$

and

$$\frac{d^2 x_\ell}{dt^2} + 2k_1 {v_d}^2 \sinh(k_1 v_d t) \sin[k_1 x_\ell(t)] = 0. \tag{49}$$

The energy conservation Equation (48) shows that, at the early stage of the instability, electrons having a positive velocity $v_\ell(t) > 0$ at a location $0 < x_\ell(t) < L_x/2$ as well as electrons having a negative velocity $v_\ell(t) < 0$ at a location $-L_x/2 < x_\ell(t) < 0$ are losing energy contrary to electrons having a negative velocity $v_\ell(t) < 0$ at a location $0 < x_\ell(t) < L_x/2$ or electrons having a positive velocity $v_\ell(t) > 0$ at a location $-L_x/2 < x_\ell(t) < 0$ that are earning energy. In order to determine such an electron trajectory according to its equation of motion (49), one can assume in addition that $k_1 x_\ell(t) \ll 1$ remains valid at every time $t > 0$ if it is valid at $t = 0$ such that $\forall t$, $\sin[k_1 x_\ell(t)] \sim k_1 x_\ell(t)$ and consider time scales of the order of electrostatic plasma oscillations ${\omega_p}^{-1}$ so that we may consider $\sinh(k_1 v_d t) \sim \exp(k_1 v_d t)/2$. In this case, (49) simplifies into

$$\frac{d^2 x_\ell}{dt^2} + (k_1 v_d)^2 \exp(k_1 v_d t) x_\ell(t) = 0. \tag{50}$$

Recognizing the differential Bessel Equation by doing the change of variable $\mathrm{v}(t) = \exp(k_1 v_d t)$

$$\frac{d^2 x_\ell}{d\mathrm{v}^2} + \frac{1}{\mathrm{v}} \frac{dx_\ell}{d\mathrm{v}} + \frac{1}{\mathrm{v}} x_\ell(\mathrm{v}) = 0, \tag{51}$$

the beam electron trajectories can be found readily. They read

$$k_1 x_\ell(t) = k_1 x_J J_0\left(2\sqrt{\mathrm{v}(t)}\right) + k_1 x_Y Y_0\left(2\sqrt{\mathrm{v}(t)}\right) \tag{52}$$

and

$$v_\ell\left(t\right) = -v_\mathrm{d}\left[k_1 x_J J_1\left(2\sqrt{\mathrm{v}\left(t\right)}\right) + k_1 x_Y Y_1\left(2\sqrt{\mathrm{v}\left(t\right)}\right)\right]\sqrt{\mathrm{v}\left(t\right)} \tag{53}$$

with

$$\left\{\begin{array}{lcl} k_1 x_J & = & +\dfrac{Y_1\left(2\right)k_1 x_0 + Y_0\left(2\right)\left(v_0/v_d\right)}{J_0\left(2\right)Y_1\left(2\right) - J_1\left(2\right)Y_0\left(2\right)} \\ k_1 x_Y & = & -\dfrac{J_1\left(2\right)k_1 x_0 + J_0\left(2\right)\left(v_0/v_d\right)}{J_0\left(2\right)Y_1\left(2\right) - J_1\left(2\right)Y_0\left(2\right)} \end{array}\right. , \tag{54}$$

accounting for the initial conditions at $t = 0$. Here, J_μ and Y_μ are the Bessel functions of the first and second kind of order μ respectively. Some of these beam electron orbits are plotted in Figure 7. We can see that the beam electrons are looping around the phase-space center $(x,\, v) = (0,\, 0)$ with a velocity amplitude increasing with their initial spatial distance from $x = 0$ in agreement with the ESVM simulation Figure 4.

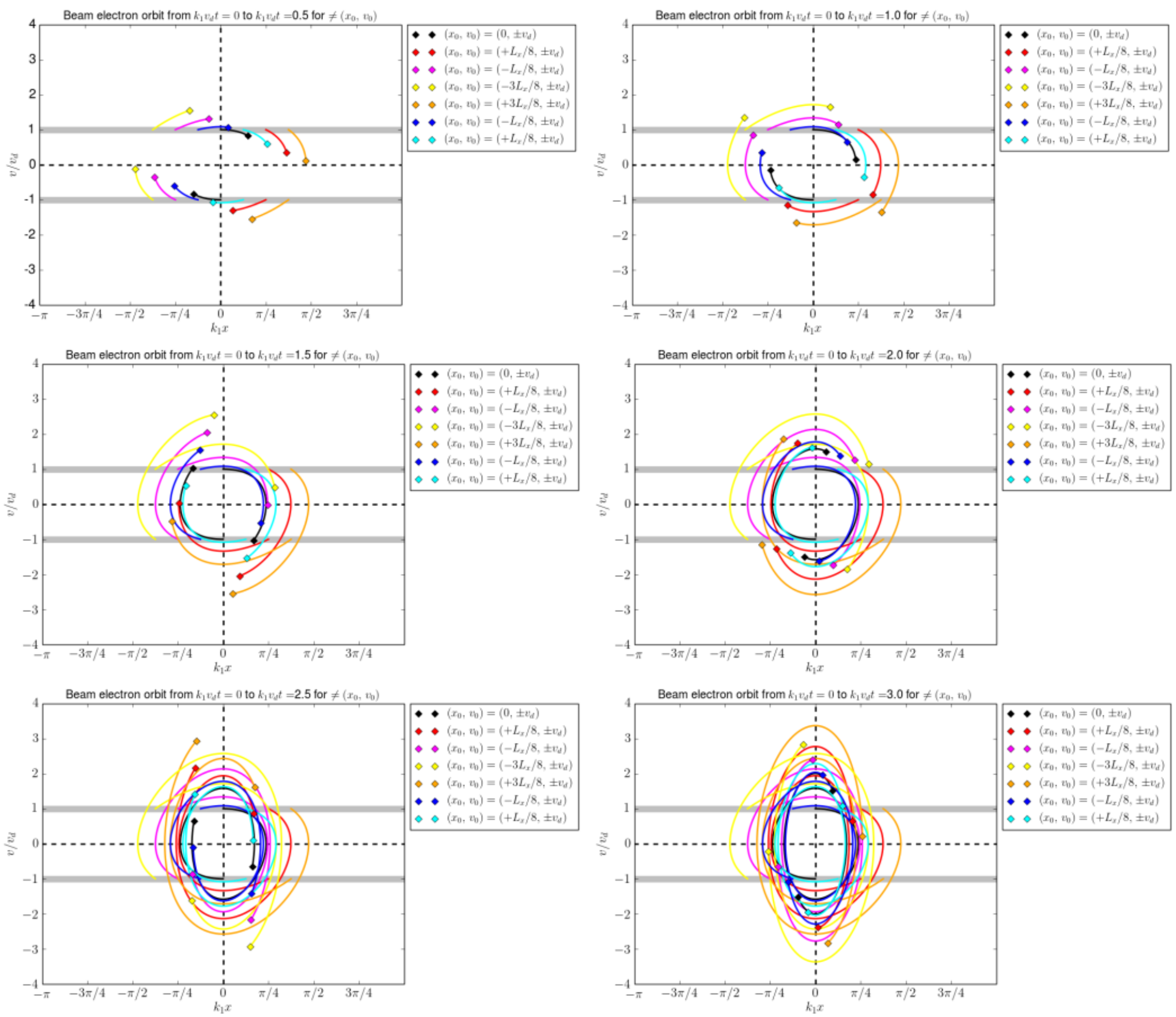

Figure 7: Two stream instability test case : Some beam electron orbits according to the analytical estimates (52) and (53).

References

[Decyk, 1987] Decyk, V. K. (1987). Simulation of microscopic processes in plasma. *Proceedings of the 1987 International Conference on Plasma Physics, Kiev, USSR, April 1987, ed. A G Sitenko [World Scientific, Singapore, 1987] vol. II, p. 1075.*

[Fried and Conte, 1961] Fried, B. D. and Conte, S. D. (1961). The Plasma Dispersion Function. Elsevier.

[Landau and Lifshitz, 1981] Landau, L. D. and Lifshitz, E. M. (1981). *Physical kinetics*, volume 10 of *A Course of Theoretical Physics*. Pergamon Press.

[Sagdeev and Galeev, 1969] Sagdeev, R. Z. and Galeev, A. A. (1969). *Nonlinear Plasma Theory*. W. A. Benjamin, Inc., New York.